Lift Development of Delta Wings Undergoing Constant Acceleration from Rest

R. Steven Sawyer*
Boeing Commercial Airplane Group, Seattle, Washington 98124
and
John P. Sullivan†
Purdue University, West Lafayette, Indiana 47906

An experimental study of two delta wings undergoing constant acceleration in forward speed has been performed. Flat plate planforms with aspect ratios of 2.29 ($\Lambda \cong 60$ deg) and 4.01 ($\Lambda \cong 45$ deg) have been tested at nominal angles of attack of 10, 20, and 30 deg for three different accelerations. Lift, as a function of time, was measured during these maneuvers. A modified von Kármán and Sears analysis suggested a nondimensionalization by which the results at different angles of attack and accelerations could be compared directly. When analyzed in this manner, the data for the aspect ratio 2.29 wing was noticeably less than predicted. This was attributed to forward movement of the leading-edge vortex burst position with acceleration, which was confirmed by flow visualization. At 10 deg, the aspect ratio 4.01 wing showed response that was well predicted by the analysis, and the upper surface flowfield was found to remain similar to the steady-state case. The poststall response for this wing was greater than predicted and, surprisingly, nonmonotonic with increasing acceleration. Flow visualization revealed that ordered structures were formed under acceleration, in contrast to the disordered wake seen at steady state.

Nomenclature

$\bar{a}$ = acceleration, ft/s^2
b = wing span, ft
C_L = wing lift coefficient, $L/(\frac{1}{2}\rho U_\infty^2 S)$
$\bar{C}_{L\alpha}$ = apparent lift curve slope, $(C_L|_\alpha)/\alpha$, 1/rad
$\bar{c}$ = mean wing chord, = ½ root chord, ft
L = wing lift, lbf
$\bar{L}$ = nondimensional wing lift, $L/[b\pi\rho\bar{c}^2\bar{a}\alpha]$
L_0 = theoretical quasisteady lift term, lbf
L_1 = theoretical apparent mass lift term, lbf
L_2 = theoretical wake effect term, lbf
$Re_{\bar{c}}$ = Reynolds number, $\rho U_\infty \bar{c}/\mu$
S = wing planform area, ft^2
t = time, s
$\bar{t}$ = nondimensional time
U_∞ = freestream speed, ft/s
α = geometric angle of attack, deg, rad
μ = dynamic viscosity, slug/ft · s
ρ = density, slug/ft^3
Φ = wing indicial response function

Introduction

FLAT plate delta wings are of interest to researchers since they readily illustrate aerodynamic phenomena that occur on more realistic aircraft configurations. This interest is heightened further by the demand for next generation fighters to perform maneuvers at very high angles of attack. Understanding their aerodynamic characteristics in unsteady situations then is of paramount importance. Although the performance of delta wings in steady flow at moderate angles of attack has been widely studied and can be predicted with a fair degree of accuracy, the behavior at high angles of attack in unsteady flows is comparatively unknown. The work here addresses some of the problems in this intriguing area.

As stated previously, delta wing response in steady flow has been widely studied. The first tests of delta wings have been credited to Winter[1] in 1935. Other experimental studies treating delta wings include those of Bartlett and Vidal[2] in 1955, Earnshaw and Lawford[3] in 1964, Wentz and Kohlman[4] in 1971, and Hummel[5] in 1978.

Such studies point out the major reason these planforms are of interest: at moderate angles of attack they produce much greater lift than would be predicted by a simple potential flow calculation. This is due to the formation of large vortical structures, referred to as leading-edge vortices, that roll up over the planform. This causes localized regions of static pressure decrease that augment the lift. These are fairly complex structures emanating from the separation line occurring at or very near the wing leading edge. Even with this complexity, fairly simple models such as the leading-edge suction analogy of Polhamus[6] or a modified vortex lattice code such as that of Katz[7] can adequately predict the lift response.

At higher angles of attack, however, the leading-edge vortices can burst. This phenomenon, due to the propagation of the vortex into a region of adverse pressure gradient, is often characterized by a sudden expansion of the vortex core, with the mutation of the vortex into a diffuse, disordered mass farther downstream (see e.g., Lambourne and Bryer[8]). Lift response is noticeably degraded if the vortices burst above the planform, yet most analyses cannot account for such occurrences. At even higher angles of attack, the flowfield suffers total breakdown and takes on the character of bluff body wake flow.

It is in these regimes that unsteady response is of interest and data are especially lacking. Much of the work to date has been flow visualization, with the studies of Gad-el-Hak and Ho[9] and LeMay et al.[10] being prime examples. Force measurements have usually been acquired for periodic situations. In 1987, Lee et al.[11] presented measured lift response for a delta wing subjected to periodic fluctuations of the freestream velocity. Den Boer and Cunningham[12,13] have measured un-

Presented as Paper 90-0310 at the AIAA 28th Aerospace Sciences Meeting, Reno, NV, Jan. 8–11, 1990; received June 30, 1990; revision received Jan. 29, 1991; accepted for publication Jan. 29, 1991.

*Senior Specialist Engineer, New Wind Tunnel Program, Box 3707, M/S 33-43. Member AIAA.

†Professor, Aerospace Sciences Laboratory, School of Aeronautics and Astronautics. Member AIAA.

steady forces and pressures for a straked delta wing undergoing a harmonic pitch oscillation.

For this current research, two flat plate delta wings with aspect ratios of 2.29 (b = 1.72 ft) and 4.01 (b = 1.98 ft) were tested. They were given constant accelerations from rest of approximately 13, 20, and 26 ft/s^2 for nominal angles of attack of 10, 20, and 30 deg. Lift and spatial position of the wings vs time for these cases have been measured. These results were compared to a modified von Kármán and Sears analysis. Additionally, flow visualization studies have been performed for these wings in both steady and accelerating flows.

Test Facilities and Experimental Technique

The majority of tests were conducted to examine the behavior of the planforms during constant acceleration from rest. Ancillary tests were also done in steady-state conditions, and both will be described briefly here.

Unsteady Tests

A sketch of the test rig for the constant acceleration tests is shown in Fig. 1. The models were mounted to four piezoquartz (PCB model 208A02) force transducers, which were in turn bolted to two pylons. These pylons were connected to a cart that moved along two parallel rails mounted on a heavy steel table. The acceleration was determined by pivoting the table to a certain angle. The motive force was merely the sine component of gravity. The cart was held against a stop at the upper end of the table, then released. The cart had 4.75 ft of travel before the brake was reached.

Position data was generated using a table mounted encoder rail and a cart mounted photodiode. This system produced characteristic voltage dropouts when cuts at known positions in the encoder rail were encountered. The output for a run was captured on one channel of a digital oscilloscope. This trace was transferred to a microcomputer that identified the time intervals between the low-voltage occurrences. Since the cut spacing was known, position vs time was therefore known. Regression fits were then used to deduce speed vs time of such results. A schematic of the position data acquisition system is shown in Sawyer and Sullivan.[14]

Force data were acquired using the system also shown schematically in Sawyer and Sullivan.[14] The individual transducer gains were adjusted to a common system gain. The gains were matched to within about 1% of the overall mean. The model/pylon structure behaved like a lightly damped second-order system, with a natural frequency of 50–60 Hz. To minimize amplitude distortion and to limit structural noise, an analog 30-Hz low-pass Butterworth filter was employed. The force data were captured using the second channel of the oscilloscope. Thus, time correlated force and position data were available. The force data were then transferred to the microcomputer for storage and postprocessing.

Normally, a number of runs were conducted at a given angle of attack and acceleration, then averaged. These were considered raw runs. At the same acceleration, a number of runs were performed with the angle of attack at 0 deg. The average of these was considered a tare. The final result was then the tare subtracted from the average of the raw runs.

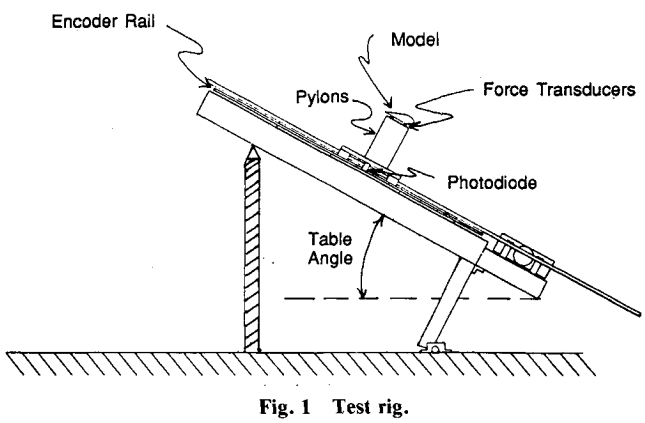

Fig. 1 Test rig.

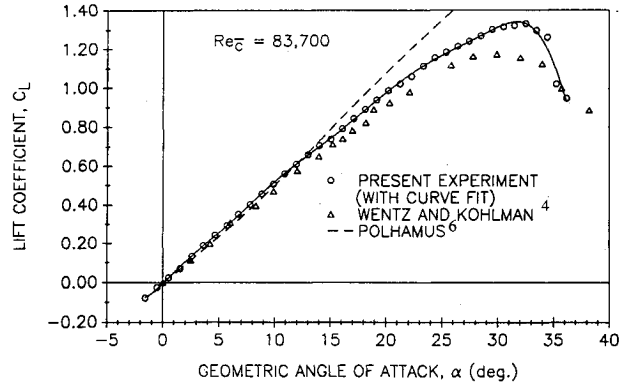

Fig. 2 Lift coefficient vs angle-of-attack results for an aspect ratio 2.29 delta wing.

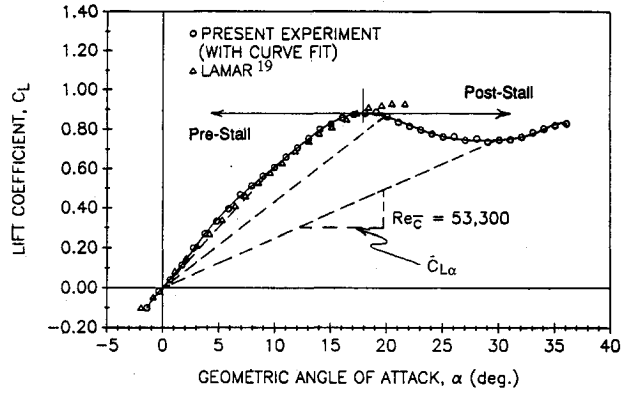

Fig. 3 Lift coefficient vs angle-of-attack results for an aspect ratio 4.01 delta wing.

Steady-State Tests

Steady-state tests were conducted in the 3.0 × 4.5 ft closed test section of the large subsonic wind tunnel at the Purdue University Aerospace Sciences Laboratory. The models were attached to a six-degree-of-freedom balance via three supports protruding through the tunnel floor. The balance was fixed with an angle of attack driver that allowed geometric angle variation between − 2 and + 35 deg. All tests were run with freestream speeds of approximately 18 ft/s.

The balance lift load cell was connected to a strain gauge conditioner. Since only steady-state data was desired, the voltage output from the conditioner was passed through a 1-Hz low-pass filter, sampled by an analog to digital converter (A/D), then processed and stored by a microcomputer. The lift channel of the balance was the only output acquired. Normally, the A/D sampled at 200 Hz for 13 s at each test condition. The data point recorded was the mean of these 2600 samples.

Actual testing was preceded by a dead weight calibration of the balance with the model mounted and the tunnel off. The tunnel was then started and allowed to warm up. Data were then acquired for the angle-of-attack range specified previously. Additionally, freestream dynamic pressure was recorded at each test point. Postprocessing included applying the calibration to the acquired voltages, yielding raw force data. These data were then corrected for flow angularity and downwash effects in a standard fashion, then normalized using wing geometry and test dynamic pressures.

Further details of the testing techniques used can be found in Sawyer.[15]

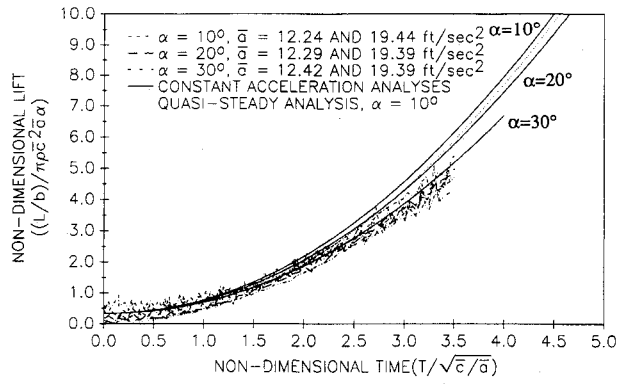

Fig. 4 Nondimensionalized unsteady lift results for an aspect ratio 2.29 delta wing.

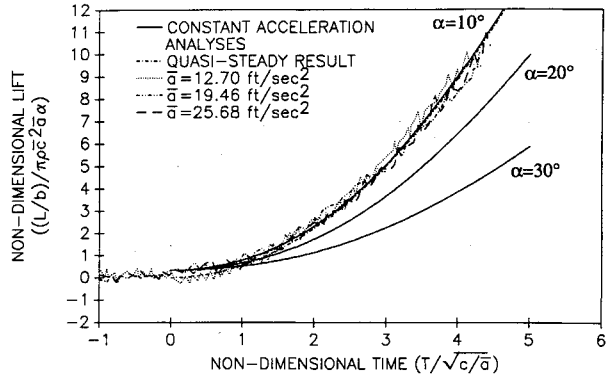

Fig. 5 Nondimensionalized unsteady lift results for an aspect ratio 4.01 delta wing at 10-deg angle of attack.

Theoretical Analysis

In 1938, von Kármán and Sears[16] produced a method by which the unsteady lift and moment of an airfoil could be calculated easily. This approach afforded numerous advantages, including applicability to any generalized motion, and the fact that the terms in the analysis were derived in such a way that they had physical significance. For the sake of discussion, the lift was comprised of three terms: L_1, the apparent mass term; L_0, the quasisteady lift contribution; and L_2, the lift-deficiency or wake effect term. The main drawback to this analysis is that extension to three dimensions is not trivial.

For constant acceleration cases, however, this extension can be accomplished easily if the spirit of the original work is maintained. For example, for constant accelerations, the L_1 term is also constant and can be evaluated by the method outlined by Batchelor.[17] The result is

$$L_1 = \tfrac{1}{3}[b\pi\rho\bar{c}^2\bar{a}\alpha]$$

The quantity in brackets occurs in the other two terms, thus suggesting a convenient nondimensionalization by which results at different geometries, accelerations, or angles of attack can be compared.

At this point, a time normalization is also introduced:

$$\bar{t} = t\sqrt{(\bar{a}/\bar{c})}$$

This is employed in the evaluation of the following two terms. Since the L_0 term is a quasisteady term, a straightforward approach by which the circulation is found from the steady-state lift can be used, thus,

$$L_0 = \left(\frac{\bar{C}_{L\alpha}}{2\pi}\right)\bar{t}^2[b\pi\rho\bar{c}^2\bar{a}\alpha]$$

The L_2 term can be attacked in a similar manner, with the result:

$$L_2 = -\left(\frac{\bar{C}_{L\alpha}\bar{t}}{2\pi}\right)[b\pi\rho\bar{c}^2\bar{a}\alpha]\int_0^{\bar{t}}\Phi[\tfrac{1}{2}(\bar{t}^2-\bar{\tau}^2)]\,d\bar{\tau}$$

For the initial von Kármán and Sears work, this was simply the Wagner function. For the analysis here, the results of Dore[18] are used. These functions can be approximated adequately by using simple polynomial fits.

$\bar{C}_{L\alpha}$ is the only quantity appearing in the L_0 and L_2 terms that is not essentially known from either the geometry of the wing or the test conditions. It can be evaluated most easily using steady C_L vs α data for the wing being tested. This was the approach used for the results presented here.

Actual calculation of the nondimensional lift is a simple marching procedure in nondimensional time, where L_2 is evaluated by numerical integration at each time step. It will be illustrated in the results that L_0, the quasisteady term, is the dominant term. It is linear in $\bar{C}_{L\alpha}$ (thus, steady-state lift coefficient as well); therefore, changes in this quantity cause noticeable changes in predicted response. With the given nondimensionalization, this analysis predicts one result for any acceleration at a given angle of attack. If the lift curve slope is also constant, the predictions will be the same for any angle of attack as well.

Results

Steady-state wing results are presented first to illustrate the source of major differences in predictions. Unsteady findings in comparison with the predictions are given next, then flow visualization results to substantiate claims about force results are given.

Steady-State Results

Figure 2 is the measured C_L vs α result for the aspect ratio 2.29 delta wing. Previous results of Wentz and Kohlman[4] and

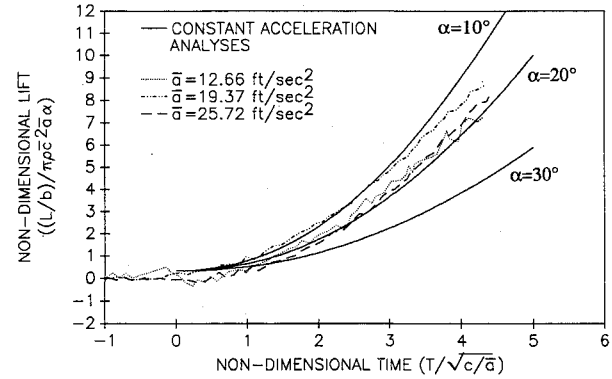

Fig. 6 Nondimensionalized unsteady lift results for an aspect ratio 4.01 delta wing at 20-deg angle of attack.

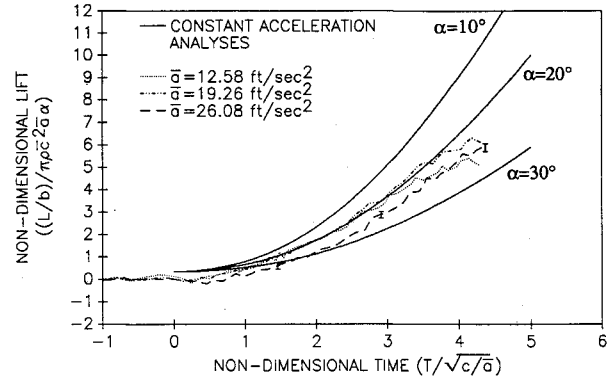

Fig. 7 Nondimensionalized unsteady lift results for an aspect ratio 4.01 delta wing at 30-deg angle of attack.

a Polhamus[6] prediction are included for comparison. Agreement is good, with the current result deviating from the prediction at 14 deg. This is approximately the angle at which the leading-edge vortex burst crosses the trailing edge of the planform.[3,4] Given the nature of the Polhamus method, this is exactly the point at which the prediction should begin to overpredict the measured results.

For discussion, stall point will be considered the first angle at which the local lift curve slope changes sign. For this wing, the stall angle is 32 deg. Thus, the three unsteady test angles are considered prestall. For this wing, $\bar{C}_{L\alpha}$ is nearly constant for prestall angles; therefore, by the discussion in the previous section, the theoretical unsteady predictions are nearly the same for all accelerations and test angles.

The aspect ratio 4.01 results (Fig. 3) show excellent agreement below stall with the data of Lamar.[19] This wing exhibits a stall angle of 18 deg. Thus, the test angle of 10 deg is considered pre-stall, while the test angles of 20 and 30 deg are considered poststall. As illustrated in Fig. 3, $\bar{C}_{L\alpha}$ decreases dramatically with increasing angle of attack. Predicted unsteady response, therefore, also decreases markedly with increasing angle.

Unsteady Results

Results for the aspect ratio 2.29 wing are shown in Fig. 4. The constant acceleration analytical predictions for the three test angles are illustrated as well. Also included is a quasi-steady analysis for the lowest test angle. This is just the nondimensionalized L_0 term of the unsteady prediction. Comparison of the quasi-steady result to the corresponding unsteady prediction immediately substantiates the earlier remark that L_0 is the dominant term of the analysis.

A number of observations about the results can be made immediately. First, experimental results for all test angles and accelerations fall into a single band. Earlier tests indicate that 26 ft/s^2 results would also fall into this band. As previously discussed, the apparent lift curve slope is nearly constant for the three test angles; thus, the collapse of the data is expected. This is illustrated by the spread of only 16% seen in the predictions.

The analyses, however, systematically overpredict the measured wing response by approximately 16% at the highest recorded time. Since the dominant L_0 term is linear in steady-state lift coefficient, it is felt that the wing is exhibiting unsteady lift coefficients less than steady-state values at the corresponding angles of attack.

A possible explanation for this behavior is available. Various researchers[3,4] have investigated the effects of leading-edge vortex bursting in steady-state tests. It is generally agreed that, if a burst occurs, it moves forward along the planform with increasing angle of attack. It is also inferred from such studies that, as more of the planform is influenced by the burst vortex, the local lift curve slope decreases. Additionally, when these planforms are given positive accelerations, other studies[8,11] have found that the burst moves forward. Lambourne and Bryer[8] claim that for a given acceleration, the burst moves to a new, fixed location. Thus, the accelerated wing would exhibit a lift coefficient lower than the steady-state value for a given angle of attack. This would cause a corresponding decrease in apparent lift curve slope and an unsteady lift response lower than predicted using steady-state values.

Aspect ratio 4.01 wing data is shown in Figs. 5–7. In contrast to the results for the aspect ratio 2.29 wing, these results do not collapse in the nondimensional space for the range of angles of attack tested. One reason for this is illustrated by the presented analytical results, which show a maximum spread of 80% due to $\bar{C}_{L\alpha}$ variations. The test angles for this wing cover prestall and poststall cases, and so apparent lift curve slope changes dramatically.

Figure 5 gives the results for various accelerations with the wing at 10 deg, the prestall case. The curves seem to collapse,

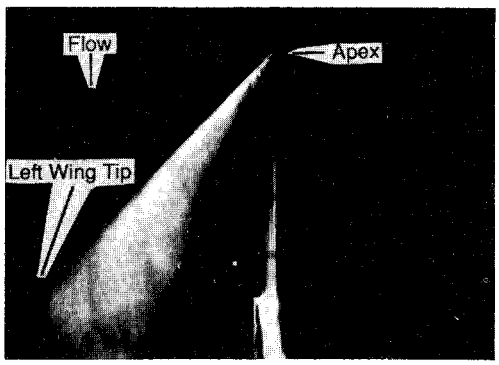

Fig. 8 Steady-state flow visualization of an aspect ratio 4.01 delta wing at 10-deg angle of attack.

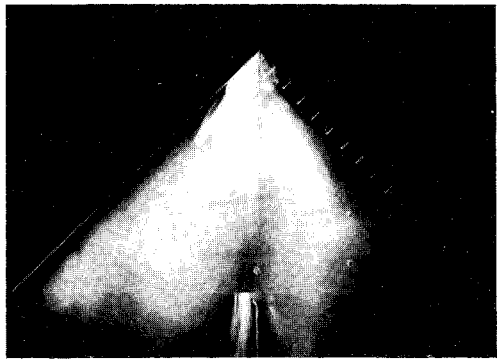

Fig. 9 Steady-state flow visualization of an aspect ratio 4.01 delta wing at 20-deg angle of attack.

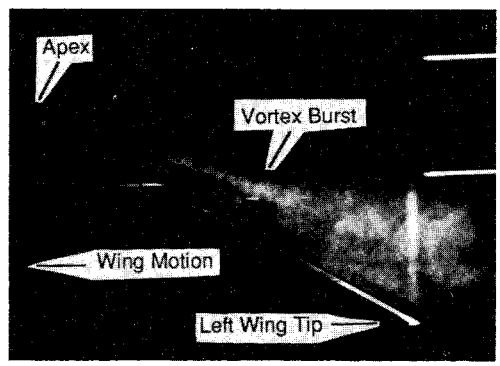

Fig. 10 Flow visualization of an aspect ratio 2.29 delta wing at an angle of attack of 10 deg and nominal acceleration of 13 ft/s^2.

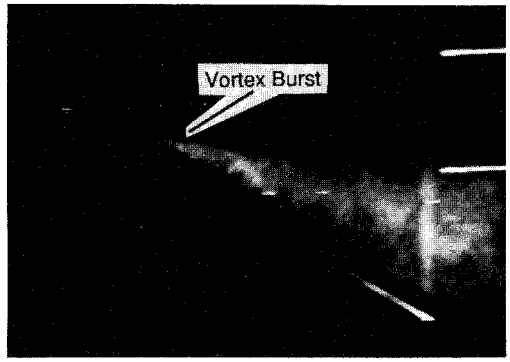

Fig. 11 Flow visualization of an aspect ratio 2.29 delta wing at an angle of attack of 20 deg and nominal acceleration of 20 ft/s^2.

with no significant spread seen between the cases. The analysis predicts the response well.

Figure 6 shows the results for the 20-deg case. For the lowest and highest accelerations, the response is nearly identical. The analytical result underpredicts the response for these two runs by about 10% at the highest recorded time. The surprising result is that, for the middle acceleration, the lift response is approximately 13% higher when compared to the response for the other two accelerations.

A similar occurrence is seen in Fig. 7 for the 30-deg case. The highest acceleration shows the lowest response, whereas, again, the middle acceleration shows the best response, 14% higher than for the high-acceleration result. The lowest acceleration follows the middle acceleration curve until a nondimensional time of 2.5, then falls to meet the high-acceleration curve. The response for all accelerations is approximately 20% higher than the analytical prediction for this angle. Parenthetically, the error bars in Fig. 7 illustrate the calculated uncertainty of these results (see Sawyer[15]).

For both 20 and 30 deg, the results are nonmonotonic with respect to acceleration, with the middle acceleration giving the most surprising response. Although both of these anomalous results were collected in the same test set, it is noted that the 10-deg case also sampled in the set did not show such behavior.

The 20- and 30-deg cases are considered poststall. It was believed that the stall point indicated a restructuring occurring in the flow over the upper surface of the wing. This would be a change from a vortical field to that of an extremely disordered wake as seen behind any flat plate normal to a flow. Tests past the stall angle deal with far different phenomena than that of a burst leading-edge vortex, for example. It was concluded that acceleration must cause significant alteration of the wake structure to greatly influence the pressure field on the wing upper surface.

Flow Visualization

An extensive flow visualization study was conducted. The purpose of this work was to identify phenomena in the flowfield causing the unusual features in the force data not predicted by the analysis. The work included studies of both the actual unsteady situation, as well as steady-state tests for comparison. In all cases, visualization was accomplished at the actual conditions for which the force data was taken. A small amount of titanium tetrachloride ($TiCl_4$) was applied to the left side of the wing apex as a marker.

Steady-State Visualization

The upper surface flowfield for both wings was investigated in the wind tunnel. Photographs were recorded at the three test angles of attack. The aspect ratio 2.29 wing exhibited classic delta wing behavior. At 10 deg, the leading-edge vortex was tightly wrapped; no burst was seen. At 20 deg, a burst occurred at about 54% of the root chord from the trailing edge. At 30 deg, the burst moved to about 85%. These observations were in agreement with those of previous researchers.[4,8]

Figures 8 and 9 illustrate the flowfield around the aspect ratio 4.01 wing at 10 and 20 deg. At 10 deg, the wing seems to exhibit an ordered vortical flow, although a single filament or core cannot be discerned. At 20 deg (and 30 deg[12]), the flow is extremely disordered in the normal sense of a separated wake. A large amount of recirculation was evident in this wake, and no readily identifiable coherent structure was seen at these conditions.

Unsteady Visualization

In the unsteady visualization figures, the upper surface flow is recorded with the apex to the left of the photograph. The bright spot normally seen in the lower right distinguishes the left wingtip.

Visualization of the accelerating aspect ratio 2.29 wing is presented in Figs. 10 and 11. Two results are immediately apparent. First, for the 10-deg case (Fig. 10), a vortex burst is seen over the wing planform. This is in marked contrast to the steady-state case, where no burst is seen.

Second, in agreement with other investigations, the burst position moves forward with increasing acceleration for all of the cases. For the 10-deg cases, the burst moves from off of the wing at steady state to 41% of root chord at 13 ft/s^2 (Fig. 10) to 51% at 20 ft/s^2 (see Ref. 14). For the 20-deg cases, the burst moves from 54% at steady state to 60% at 13 ft/s^2 (see Ref. 14) to 68% at 20 ft/s^2 (Fig. 11). The burst at 30 deg, identified at 85% in the steady state, seems to be at or very near the apex for both accelerations (see Sawyer and Sullivan[14]).

These findings indicate that a large displacement of the burst point can occur under acceleration, in contrast to the claims of Lee et al.[11] As discussed earlier, the appearance of a vortex burst over the planform is normally associated with degraded wing performance. The flow visualization reinforces the earlier suggestion that unsteady lift response of the aspect

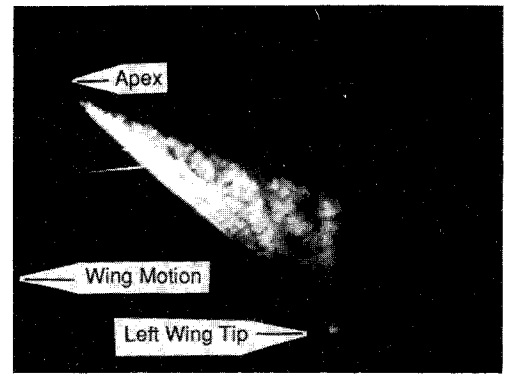

Fig. 12 Flow visualization of an aspect ratio 4.01 delta wing at an angle of attack of 10 deg and nominal acceleration of 26 ft/s^2.

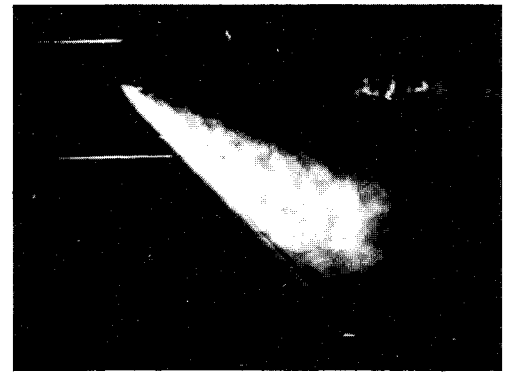

Fig. 13 Flow visualization of an aspect ratio 4.01 delta wing at an angle of attack of 20 deg and nominal acceleration of 26 ft/s^2.

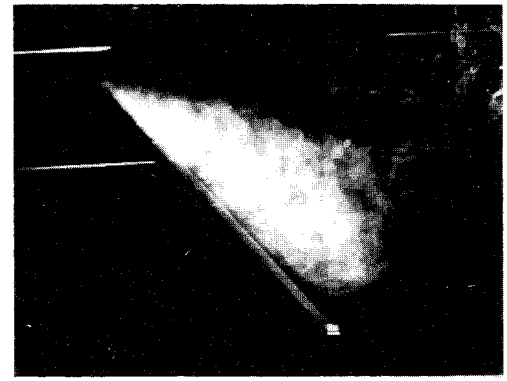

Fig. 14 Flow visualization of an aspect ratio 4.01 delta wing at an angle of attack of 30 deg and nominal acceleration of 26 ft/s^2.

ratio 2.29 wing is lower than predicted due to the forward movement of the burst with acceleration.

Unsteady flow visualization of the aspect ratio 4.01 wing is illustrated in Figs. 12–14. Examples at other conditions can be found in Sawyer and Sullivan.[14] A result for this wing at 10 deg is shown in Fig. 12. The structure visualized is qualitatively similar to that seen in the steady-state case. However, its physical size seems to decrease monotonically for increasing acceleration.

A 20-deg result is shown in Fig. 13. A coherent structure is formed as the wing is accelerated, in obvious contrast with the steady-state result, Fig. 9. This structure also decreases in size with increasing acceleration. The 30-deg cases, illustrated by Fig. 14, are similar to the 20-deg results. Again, structure is seen with a decrease in size with increasing acceleration.

Visualizations by Freymuth[20,21] seem to be in agreement with these findings. He observed vortical structures forming on the suction side of an accelerating delta wing operating at angles above the static stall angle. As pointed out here (but not noted in previous studies), this is in contrast with the bluff body wake flow that would be expected in the steady state.

A number of important points can be drawn from the visualization. For the 10-deg cases, the size of the structure seen seems only slightly altered under acceleration. The agreement between the force data and the analysis is therefore considered reasonable.

For the 20- and 30-deg cases, upper surface flow is radically different than that observed in the steady state. It is believed that the formation of such structures favorably affects the pressure field; there is certainly no longer any large recirculating regions behind the wing. This is in agreement with the finding that in all cases the unsteady lift response is higher than predicted.

The size of these structures varies greatly.[14] Certainly, structure size may be nothing more than a result of the fact that, for a given position along the rails, higher accelerations create higher speeds. However, it is stressed that the sizes show monotonic decreases with increasing acceleration, whereas the lift displays a nonmonotonic behavior. It is also recognized that changes in force on the wing will be a function of not only the location or size of the structure, but its strength (in the sense of circulation) as well. The current tests furnish no information about the latter.

Conclusions

Two delta wings with aspect ratios of 2.29 and 4.01 have been examined in both steady and accelerating flows. Results from the steady-state tests, both lift data and flow visualization, agree favorably with previous studies.

Unsteady lift response for the aspect ratio 2.29 wing collapses to a single band in the chosen nondimensional space for all angles of attack and accelerations. A modified von Kármán and Sears analysis overpredicts the overall wing response. This is attributed to the movement of the leading-edge vortex burst point with acceleration. Flow visualization in the accelerating flow indicates that the amount of movement is significant.

Aspect ratio 4.01 unsteady results show qualitatively different behavior for prestall and poststall cases. For the prestall case ($\alpha = 10$ deg), results for all accelerations collapse to one curve, which is predicted well by the analysis.

In all cases, the poststall tests ($\alpha = 20$ and 30 deg) produce noticeably higher lift values than those predicted analytically. Additionally, the force data show significant nonmonotonic behavior with increasing acceleration. Such character is not predicted by the analysis.

Results from flow visualization indicate that ordered structures are formed under acceleration, in marked contrast to the disordered wake seen in the steady state. The improved lift response is attributed to these formations. These structures decrease in size with increasing acceleration. Although the lift response does not show such a monotonic behavior, it is noted that the flow visualization only furnishes information about the size of these structures, not strength. This illustrates the flow complexity and points to the need for surface pressure distribution or flowfield measurements to help to understand this situation fully.

References

[1]Winter, H., "Strömungsvorgange an Platten und Profilierten Körpern beil Kleinen Spannweiten," *Forschung auf dem Gebiete des Ingenieur-Wesens,* Vol. 6, No. 2, 1935, pp. 67–71.

[2]Bartlett, G. E., and Vidal, R. J., "Experimental Investigation of Influence of Edge Shape on the Aerodynamic Characteristics of Low Aspect Ratio Wings," *Journal of the Aeronautical Sciences,* Vol. 22, No. 8, 1955, pp. 517–533, 588.

[3]Earnshaw, P. B., and Lawford, J. A., "Low-Speed Wind-Tunnel Experiments on a Series of Sharp-Edged Delta Wings," British Aeronautical Research Council, Reports and Memoranda, No. 3424, London, March 1964.

[4]Wentz, W. H., Jr., and Kohlman, D. L., "Vortex Breakdown on Slender Sharp-Edged Wings," *Journal of Aircraft,* Vol. 8, No. 3, 1971, pp. 156–161.

[5]Hummel, D., "On the Vortex Formation over a Slender Wing at Large Angles of Incidence," *High Angle of Attack Aerodynamics,* Paper 15, AGARD CP-247, Oct. 1978.

[6]Polhamus, E. C., "Predictions of Vortex-Lift Characteristics by a Leading Edge Suction Analogy," *Journal of Aircraft,* Vol. 8, No. 4, 1971, pp. 193–199.

[7]Katz, J., and Kern, D., "Effect of Vertical Ejector-Jet on the Vortex Lift of Delta Wings," 1st National Fluid Dynamics Congress, AIAA Paper 88-3842, Cincinnati, OH, July 1988.

[8]Lambourne, N. C., and Bryer, D. W., "The Bursting of Leading Edge Vortices—Some Observations and Discussions of the Phenomenon," British Aeronautical Research Council, Reports and Memoranda, No. 3282, London, April 1961.

[9]Gad-el-Hak, M., and Ho, C.-M., "The Pitching Delta Wing," *AIAA Journal,* Vol. 23, No. 11, 1985, pp. 1660–1665.

[10]LeMay, S. P., Batill, S. M., and Nelson, R. C., "Leading Edge Vortex Dynamics on a Pitching Delta Wing," AIAA Paper 88-2559, 6th Applied Aerodynamics Conference, Williamsburg, VA, June 1988.

[11]Lee, M., Shih, C., and Ho, C.-M., "Response of a Delta Wing in Steady and Unsteady Flow," Forum on Unsteady Flow Separation, ASME Fluids Engineering Division, Vol. 52, 1987, pp. 19–24.

[12]Den Boer, R., and Cunningham, A., "Low-Speed Unsteady Aerodynamics of a Pitching Straked Wing at High Incidence—Part I: Test Program," *Journal of Aircraft,* Vol. 27, No. 1, 1990, pp. 23–30.

[13]Cunningham, A., and den Boer, R., "Low-Speed Unsteady Aerodynamics of a Pitching Straked Wing at High Incidence—Part II: Harmonic Analysis," *Journal of Aircraft,* Vol. 27, No. 1, 1990, pp. 31–41.

[14]Sawyer, R. S., and Sullivan, J. P., "Lift Development of Delta Wings Undergoing Constant Acceleration From Rest," AIAA Paper 90-0310, Jan. 1990.

[15]Sawyer, R. S., "Measurement of Lift Development on Rapidly Accelerated Wings," Ph.D. Dissertation, Purdue Univ., West Lafayette, IN, May 1989.

[16]Von Kármán, T., and Sears, W. R., "Airfoil Theory for Non-Uniform Motion," *Journal of the Aeronautical Sciences,* Vol. 5, No. 10, 1938, pp. 379–390.

[17]Batchelor, G. K., *An Introduction to Fluid Dynamics,* Cambridge Univ. Press, Cambridge, England, UK, 1967, pp. 407–409.

[18]Dore, B. D., "The Unsteady Forces on Finite Wings in Transient Motion," British Aeronautical Research Council, Reports and Memoranda, No. 3456, London, Sept. 1964.

[19]Lamar, J. E., "Recent Studies of Subsonic Vortex Lift Including Parameters Affecting Stable Leading-Edge Vortex Flow," *Journal of Aircraft,* Vol. 14, No. 12, 1977, pp. 1205–1211.

[20]Freymuth, P., "Visualizing the Combined System of Wing Tip and Starting Vortices," TSI Flow Lines, TSI Inc., St. Paul, MN, May 1986.

[21]Freymuth, P., "Flow Visualization as a Challenge to and as a Reference for Computer Modellers," *Numerical and Applied Mathematics,* edited by W. F. Ames and J. C. Baltzer, 1989, pp. 231–236.